JOURNAL OF CATALYSIS 65, 253–262 (1980)

Carbon Deposition and Activity Changes over FeRu Alloys during Fischer–Tropsch Synthesis

G. L. OTT,[1] T. FLEISCH,[2] AND W. N. DELGASS

School of Chemical Engineering, Purdue University, West Lafayette, Indiana 47907

Received December 19, 1979; revised March 31, 1980

The interaction of $3H_2/CO$ at 1 atm and 573 to 673°K with unsupported Ru, Fe, and RuFe alloy powders was investigated using X-ray photoelectron spectroscopy, secondary ion mass spectrometry, and differential chemical kinetics. Direct surface analysis of fresh, reacted, and regenerated surfaces, without exposure to air, shows a strong dependence of carbon deposition on catalyst composition. Pure Ru and Ru doped with 3 atom% Fe show no carbon buildup, and therefore exhibit steady specific activity and selectivity in Fischer–Tropsch synthesis as a function of time on stream. Increasing the iron content of the alloys results in a thick carbon overlayer being deposited during the first few hours of reaction. The carbon overlayer reduces specific activity by a factor of 2 to 3 and shifts selectivity toward lower-molecular-weight products. Regeneration of these catalysts requires heating in H_2 at 683°K. Both XPS and SIMS confirm that pure iron first incorporates carbon into the bulk with a resulting temporary increase in activity and selectivity to saturated products. Selectivity then shifts to lighter products as carbon gradually builds up on the iron carbide surface.

INTRODUCTION

In a previous paper, it was shown that the surface of unsupported FeRu alloy powders is significantly enriched in Fe and that introduction of small amounts of Fe into an Ru surface alters the electronic nature of the catalyst (*1*). The surface composition and electronic state are reflected in the initial total hydrocarbon selectivity and the selectivity to unsaturated products in the hydrogenation of CO at 1 atm and 573°K. Using methodology similar to that of the previous paper, we focus here on the alteration of the various alloy surfaces as Fischer–Tropsch synthesis proceeds.

The interaction of CO with metal surfaces has been the subject of much research. Fuggle *et al.* (*2*) have shown that adsorption of CO on Ru(0001) is nondissociative at 295°K. They also report that an adsorbed layer of CO may dissociate due to electron beam interactions (*3*). Singh and Grenga (*4*) have shown that CO dissociates at the low-index poles of a ruthenium single crystal at temperatures above 823°K. Such behavior has been observed for nickel also where rough surfaces have proven more effective for CO dissociation than close-packed planes (*5*).

Low and Bell (*6*) and McCarty and Wise (*7*) have shown that dissociative adsorption of CO occurs at temperatures above 350°K on alumina-supported Ru. Rabo *et al.* (*8*) show dissociation of CO on silica-supported Ru at 673°K. Supported catalysts also show evidence of carbon deposition during Fischer–Tropsch synthesis in the 500°K temperature region (*9, 10*).

Iron has been shown to dissociate CO at lower temperatures. Studies of the Fe(110) surface show that CO adsorbs molecularly at room temperature but dissociates in about 1 hr. At 385°K, the dissociation is immediate (*11*). Other results confirm dissociative adsorption of CO on iron crystals at ca. 300°K (*12, 13*). On polycrystalline Fe, the adsorption is reported as dissociative at room temperature but molecular at 110°K (*14, 15*). Investigations of CO ad-

[1] Present address: Amoco Oil Co., Naperville, Ill. 60540.

[2] Present address: Standard Oil of Indiana, Naperville, Ill. 60540.

0021-9517/80/100253-10$02.00/0

sorption on polycrystalline Fe using secondary ion mass spectrometry have shown dissociative adsorption at room temperature (*16, 17*). Thus, the tendency to dissociate CO is greater for Fe than Ru, but at Fischer–Tropsch reaction temperature both metals adsorb CO dissociatively.

In addition to the variations in adsorptive behavior of Fe and Ru for CO, the interaction of carbon with these materials in the bulk is also different. There are no stable bulk carbides of Ru or FeRu alloys reported in the literature. Therefore, one would expect the carbon formed on the surface of an Ru or RuFe catalyst to either remain at the surface or be incorporated into the products. Fe, on the other hand, can form several bulk carbide phases upon heating in CO (*18*). While the particular carbide phase formed can depend on the nature of the catalyst (*19–21*), one would expect unsupported Fe powder to be able to accept surface carbon into the bulk to form the stable χ or Hägg carbide.

Thus, we can anticipate increasing propensity toward carbon formation as the iron content of RuFe alloys increases, and iron carbide formation for pure iron. We report here direct observation of these effects using X-ray photoelectron spectroscopy (XPS) and secondary ion mass spectrometry (SIMS) of high-surface-area alloy powders used as catalysts at 573°K and an H_2/CO ratio of 3.3.

EXPERIMENTAL

Surface analysis of the reacted samples was done by first parking the sample and holder in a glass chamber which allows pretreatment in 1 atm of gas at temperatures up to 773°K (*1*). After the reduction and reaction periods, the chamber was pumped to less than 10^{-4} Pa and the sample transferred in vacuum to the XPS or SIMS chamber via magnetic drive rods. XPS measurements were made with a Hewlett–Packard 5950A spectrometer, calibrated by assigning Au $4f_{7/2}$ = 84.0 eV. The SIMS instrument is comprised of a Danfysik ion delivery system, a Perkin–Elmer Ultek TNB-X bell jar, and a Riber Q156 quadrupole mass analyzer. The samples were pressed disks 7 mm in diameter and 1 mm thick. The system and procedures are described in further detail in (*22–24*).

Kinetic analysis of the catalyst powders was done at 1 atm in a fixed-bed, flow reactor (*25*) operated differentially at conversions below 3%. The product analysis was accomplished with a Hewlett–Packard Model 5834A reporting gas chromatograph with He carrier gas, a Chromosorb 102 column, and thermal conductivity detection. Calibration and operating details are given in (*25*).

Fe, Ru, and FeRu powders were prepared from $RuCl_3 \cdot H_2O$ (Englehard) and $Fe(NO_3)_3 \cdot 9H_2O$ (Mallinckrodt) by hydrazine reduction (*26*) as described previously (*27*). Both kinetic and surface analysis samples were reduced overnight in flowing UHP H_2 at 673°K before reactions were started.

RESULTS AND DISCUSSION

This section is divided into three parts commensurate with the behavior of the catalysts with respect to carbon deposition during Fischer–Tropsch synthesis. The first category, comprised of pure Ru and 97Ru3Fe, shows no detectable carbon buildup on the surface during reaction. The second group includes the 75Ru25Fe and 33Ru67Fe catalysts which show a very rapid buildup of surface carbon. The third category is the pure-iron catalyst which exhibits both formation of a bulk carbide phase and surface carbon buildup.

1. Pure Ru and 97Ru3Fe

XPS spectra of the Ru 3*d* and Fe 2*p* regions of reduced Ru and 97Ru3Fe catalysts are unchanged after reaction at 573°K for 24 hr in $3.3H_2/CO$. Both the Fe and the Ru in the samples remain zero valent and no buildup of carbon on the surface is observed. The analysis for carbon requires special care because of the overlap of the C

1*s* and Ru $3d_{3/2}$ peaks. Our procedure is to measure the intensity of the Ru $3d_{5/2}$ peak at 280 eV and subtract 0.67 of this value, attributable to Ru $3d_{3/2}$, from the peak at 284 eV. The difference is then the C 1*s* intensity at 284 eV. Because the cross-section ratio for Ru $3d_{3/2}$ vs C 1*s* is 5.1 (*28*), XPS is less sensitive to carbon than Ru and the practical lower limit of detectability for our procedure is about 0.25 monolayer of carbon. We claim, therefore, that there is less than 0.25 monolayer of carbon on the surface of the Ru and 97Ru3Fe catalysts after 24 hr of Fischer–Tropsch synthesis at 573°K.

The lack of significant carbon buildup on these samples is reflected in their kinetic performance. The overall rate of CO conversion on pure-ruthenium powder decreased by 40% in the first 3 hr of reaction, that on 97Ru3Fe decreased 20% in 2½ hr. X-Ray diffraction analysis of the Ru catalyst before and after reaction showed, however, an increase in average particle size corresponding to a 30% loss of surface area. Thus, the absolute rate per surface metal atom remains essentially unchanged and deactivation due to carbon coverage of the surface is minimal. The lack of significant carbon incorporation onto the surface is also evidenced in Table 1 by the small standard deviations in the selectivity values for the Ru and 97Ru3Fe catalysts during the first 4 hr of reaction. The higher standard deviations for higher hydrocarbon selectivities reflect approach to the lower detectability limit of the gc analysis.

The behavior of the Ru powder is consistent with the relatively high capacity of Ru for H_2 adsorption in the presence of CO at lower temperatures (*29*), but offers an interesting contrast to Ru/SiO_2 which maintains a carbon reservoir equivalent to several monolayers during reaction (*10*). As has been noted earlier (*1*), the change in selectivity with addition of 3% Fe to the bulk suggests a lowering of the hydrogen coverage and an increase in the coverage and residence time of carbon intermediates

TABLE 1

Selectivity of 100Ru and 97Ru3Fe in the First 4 hr of Reaction at 573°K in $3.3H_2/CO$[a]

Product	100Ru		97Ru3Fe	
	S_{C_n}	σ (%)	S_{C_n}	σ (%)
CO_2	0.01	4.1	0.06	18
C_1	0.85	0.8	0.55	4.1
C_2	0.08	6.2	0.25	5.3
C_3	0.05	14	0.10	16.5
C_4	—	—	0.03	18.7
Ethylene/C_2	0.31	4.5	0.87	2.7
Propylene/C_3	0.79	5.2	0.99	—

[a] S_{C_n} = fraction of CO converted which goes to the product indicated. σ = standard deviation of measurements made over the reaction period.

just large enough to enhance C_2 production. The composition of the surface producing this unique product distribution is 10 to 40% iron (*1*) and is unchanged after reaction.

2. *75Ru25Fe and 33Ru67Fe*

Recalling that no stable bulk carbides of FeRu have been reported in the literature and that the tendency for production of carbon from CO will increase with increasing Fe content, one might expect the 75Ru25Fe and 33Ru67Fe catalysts to exhibit carbon buildup on the surface.

Figure 1 shows the Ru 3*d*–C 1*s* region of the XPS spectrum of the 75Ru25Fe alloy after H_2 reduction, 1 hr of reaction at 573°K, and 4 hr of reaction at 613°K. As can be seen from the increasing relative intensity of the 284-eV peak the buildup of carbon on the surface with increasing exposure to reaction is tremendous. This rapid accumulation of carbon is also reflected in the secondary ion yields from the surfaces as presented in Fig. 2. The ions corresponding to Fe and Ru are almost completely absent after only 1 hr of reaction. SIMS, a first-monolayer technique (*30, 31*), does not see underlying metal atoms while XPS, with its greater sampling depth, does.

A semiquantitative description of the

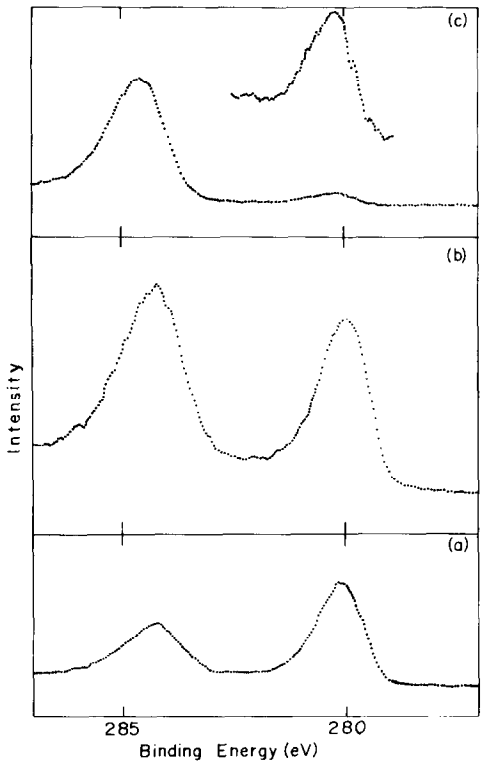

FIG. 1. Carbon buildup on 75Ru25Fe during Fischer–Tropsch synthesis as measured by XPS: (a) reduced; (b) $3H_2/CO$, 1 hr, 573°K; (c) $3H_2/CO$, 4 hr, 613°K (inset intensity × 10). Ru $3d_{5/2}$ has $E_b \cong 280$ eV while both C 1*s* and Ru $3d_{3/2}$ occur at $E_b \cong 284$ eV.

amount of carbon on the surface can be gained from a model for the relative intensity of the Ru $3d_{5/2}$ and C 1*s* XPS lines. Using the intensity equations from (*32*), assuming that the carbon is a uniform layer of thickness l over an infinitely thick slab of FeRu, and using mean free paths (*33*) of 15.8 Å for C 1*s* electrons in carbon and 13.6 Å for both Fe $2p_{3/2}$ and Ru $3d_{5/2}$ electrons in carbon and 11.6 Å for those electrons in the alloy, one can relate $(I_C/\sigma_C)/(I_{Fe}/\sigma_{Fe} + I_{Ru}/\sigma_{Ru})$ to l. For the Hewlett–Packard spectrometer with a 38° electron takeoff angle the equation is

$$(I_C/\sigma_C)/(I_{Fe}/\sigma_{Fe} + I_{Ru}/\sigma_{Ru}) = 1.83\,(1 - \exp(-0.103l))/\exp(-0.119l).$$

The cross sections are taken from Scofield (*28*). By fitting the observed relative intensities to the equation, one can estimate the equivalent thickness of the carbon layer. The results of the calculations are presented in Table 2. If the different mean free paths for Fe $2p_{3/2}$ and Ru $3d_{5/2}$ electrons are also accounted for in the model, the average metal surface layer composition can be estimated from the Fe $2p_{3/2}$ and Ru $3d_{5/2}$ relative intensities. This analysis shows that after reaction the surface composition of 75Ru25Fe is unchanged while that of 33Ru67Fe is slightly more iron rich.

Comparison of runs 1 and 6 for 75Ru25Fe shows that less carbon is deposited on the surface after 5 hr at 548°K than in 1 hr at 573°K, indicating a strong temperature dependence on the rate of carbon deposition. Run 8, for 24 hr at 613°K, indicates that the buildup of carbon on the surface does not continue forever but stops when the equivalent layer thickness is about 40 Å. The behavior of the 33Ru67Fe catalyst is similar to that of 75Ru25Fe.

The removal of the carbon overlayer is depicted in Fig. 3. As can be seen, once the overlayer is generated, the removal rate in flowing H_2 is negligible at temperatures up to 593°K. Low reactivity of overlayer carbon on iron has also been reported by Matsumoto and Bennett (*34*). By heating the catalyst to 683°K in flowing H_2, however, the fresh metal surface is regenerated.

The rapid buildup of carbon to very high

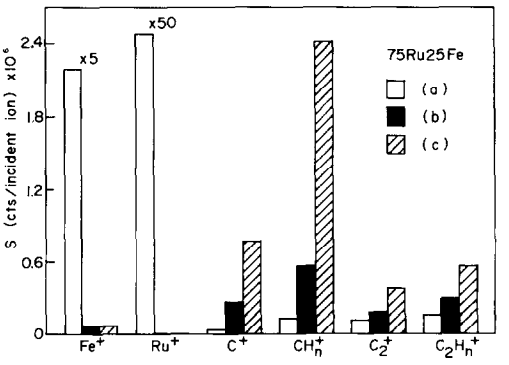

FIG. 2. Carbon buildup on 75Ru25Fe during Fischer–Tropsch synthesis as measured by SIMS: (a) reduced; (b) $3H_2/CO$, 1 hr, 573°K; (c) $3H_2/CO$, 4 hr, 613°K.

TABLE 2

Carbon Buildup as Measured with XPS on 75Ru25Fe and 33Ru67Fe as a Function of Pretreatment

Run No.	Time (hr)	Pretreatment		After run No.	$(I/\sigma)_C$ / $(I/\sigma)_{Ru} + (I/\sigma)_{Fe}$	l (Å)
		Gas	T (°K)			
			75Ru25Fe			
1	1.0	$3H_2/CO$	573	—	3.99	10
2	4.0	$3H_2/CO$	593	—	73.0	31
3	4.0	H_2	593	2	70.4	31
4	12.0	H_2	603	3	59.9	30
5	12.0	H_2	683	4	0	0
6	5.0	$3H_2/CO$	548	5	2.4	7
7	12.0	H_2	548	6	1.3	5
8	24.0	$3H_2/CO$	613	7	219	40
9	4.0	$3.3H_2/CO$	573	(from kinetics		
+	2.5	H_2	573	experiment—		
+	1.5	$3.3H_2/CO$	573	exposed to air)	6.3	13
			33Ru67Fe			
1	1.0	$3H_2/CO$	573		2.2	7
	4.0	$3H_2/CO$	613		201	40
	5.5	$3.3H_2/CO$	573	(after kinetics experiment)	7.8	14

levels and the slow regeneration rate at reaction temperature are reflected in the kinetic behavior of the materials. The lower curve in Fig. 4 shows the total hydrocarbon synthesis activity of a 75Ru25Fe catalyst as a function of time on stream in a $3.3H_2/CO$ mixture at 573°K. The catalyst was activated by H_2 reduction at 603°K overnight. In the first 4 hr of reaction time, the total rate declined by a factor of 4. Some of the activity loss may be attributable to metal sintering, but based on particle size from X-ray diffraction line broadening, at least half of the loss of activity is due to carbon deposition. After 4 hr of reaction an attempt was made to regenerate the surface in hydrogen at reaction temperature. The XPS results in Table 2, runs 2, 3, 4, show that only minimal carbon is removed during such a treatment. Figure 4 shows, commensurate with the XPS findings, that synthesis activity recovered only slightly after reintroduction of the syngas.

The upper curve in Fig. 4 shows the total hydrocarbon synthesis activity as a function of time on stream in $3.3H_2/CO$ at 617°K with attendant regeneration at 683°K. Prior to the run, the catalyst was reduced in H_2 at 673°K in order to "presinter" it. By presintering, we hoped to minimize the surface area loss of the catalyst in the higher-temperature regeneration attempt. Because of the surface area loss in pretreatment, the initial rate at 617°K is approximately half the initial rate at 573°K instead of the expected factor of 2–4 higher. The rate of deactivation is faster at 617°K than at 573°K, in keeping with the observed temperature dependence on the rate of carbon deposition.

Comparison of the curve in Fig. 4 and runs 4 and 5 of Table 2 shows that the carbon can be removed by heating in hydrogen at 683°K, and that upon removal the synthesis activity is restored.

In contrast to the pure-Ru and 97Ru3Fe catalysts, the 75Ru25Fe and 33Ru67Fe catalysts exhibit drastic changes in selectivity due to the deposition of carbon on the surface. Figure 5 shows the dependence of selectivity for the 75Ru25Fe catalyst with time on stream in $3.3H_2/CO$ at 617°K be-

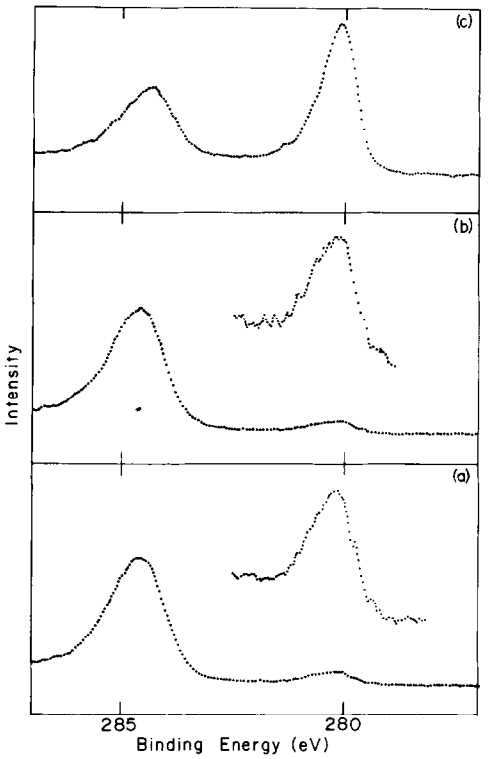

FIG. 3. Removal of carbon from 75Ru25Fe as measured by XPS: (a) $3H_2/CO$, 4 hr, 613°K; (b) H_2, 4 hr, 593°K; (c) H_2, 12 hr, 683°K (insets in (a) and (b) are intensity × 10). Ru $3d_{5/2}$ has $E_b \cong 280$ eV while both C 1*s* and Ru $3d_{3/2}$ occur at $E_b \cong 284$ eV.

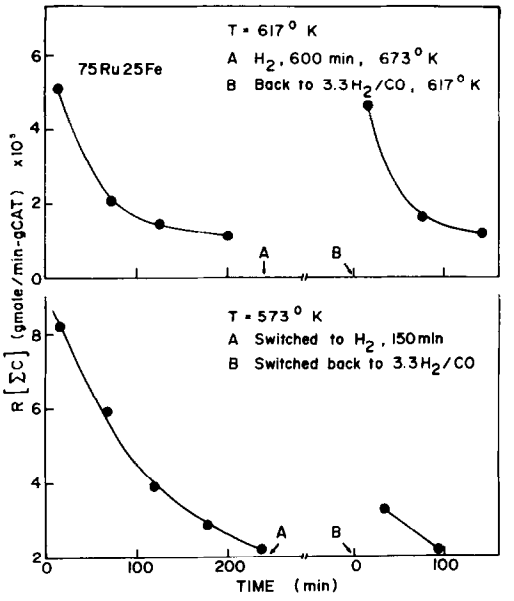

FIG. 4. Hydrocarbon synthesis activity of 75Ru25Fe versus time on stream. Lower curve: Reaction and regeneration at 573°K; upper curve: reaction at 617°K and regeneration at 683°K.

fore and after regeneration. These selectivities correspond to the total activity curves presented in the upper curve in Fig. 4. The selectivity of the catalyst shifts sharply toward C_1 products as the buildup of carbon proceeds. There is also a slight increase in the selectivity of CO_2 and a decrease in the selectivity to higher hydrocarbons. Upon regeneration of the catalyst surface by the high-temperature treatment in hydrogen, the original selectivities are restored and the deactivation process begins all over. A slight decrease in ethylene selectivity from 0.93 to 0.8 is also observed as the carbon overlayer builds up. This change is significant because lower conversion usually increases olefin to paraffin ratios (*25, 35*).

The rapid decline in synthesis activity can be attributed to a decrease in the number of active sites on the surface due to coverage with carbon. The overall decrease in activity is only a factor of 5 when the carbon overlayer measured with XPS is equivalent to more than 10 monolayers and the visibility of metal atoms in the SIMS measurement is low. This suggests that the buildup of carbon is nonuniform on the surface and that a fraction of the metal sites remain essentially uncontaminated. This would explain the approach to a steady-

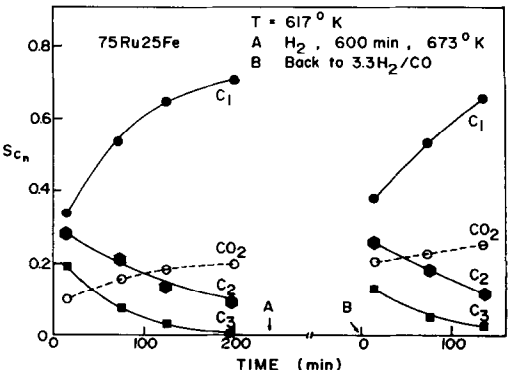

FIG. 5. Hydrocarbon selectivity of 75Ru25Fe versus time on stream during reaction at 617°K.

state overlayer thickness. Apparently, on the pure-Ru and 97Ru3Fe catalysts, the rate of carbon removal is sufficient to maintain a low coverage of carbon on the surface. For 75Ru25Fe, the following model explains the results. On the fresh 75Ru25Fe catalysts, the rate of removal is insufficient to keep carbon from depositing. As the carbon deposits, the rate of removal declines and the carbon buildup proceeds. Finally, the rate of deposition slows to the point where removal by a small very active portion of the surface compensates for the deposition and a steady state is achieved. Regeneration attempts at reaction conditions only clean the active centers but do not attack the carbon deposited on the balance of the surface. At high temperatures, the rate of attack on the balance of carbon is sufficiently enhanced to create more active centers for dissociative adsorption of hydrogen which in turn can serve to further regenerate the catalyst. Thus, there appears to be a critical Fe content in the surface (between 3 and 25 mole%) above which carbon overlayers are formed, and a critical temperature (between 603 and 683°K) of regeneration in hydrogen above which the carbon layers are removed.

The change in selectivity with carbon layer buildup is consistent with the assumption that sites for higher-hydrocarbon production require the largest metal-atom ensembles. Thus, as carbon deposition poisons large ensembles, the product distribution shifts toward methane.

In closing this discussion we note that the uniform-layer model used to estimate carbon layer thickness is not consistent with the patchy-surface model required by the kinetic behavior. While the values of the carbon layer thickness are not accurate, the relative values serve as a qualitative indicator of carbon buildup. Furthermore, the results on the alloys and on pure Fe show clearly that significant amounts of relatively unreactive carbon coexist with the true reaction intermediates. Thus, detailed analysis of rates of carbon deposition and removal should deal individually with the various types of carbon present.

3. *Pure Iron*

Carbon deposited on the surface can enter the product stream, build up on the surface, or, as is the case for iron at unsteady state, penetrate into the bulk. Fischer and Dilthey (*36*) originally proposed the possibility of incorporation of carbon into the fused iron catalyst during Fischer–Tropsch synthesis. Carbiding of iron during synthesis is now well known (*18, 19*). Recent studies of supported iron using the Mössbauer effect show effects of particle size and support on the iron carbide phase formed (*20, 21*) and also demonstrate an increase in activity corresponding to very fast carbon uptake in the bulk followed by a loss in activity after the bulk is saturated with carbon (*37*).

Figure 6 shows a similar trend for iron powder. The upper curve in Fig. 6 gives the relative intensity, normalized for photoelectric cross section and kinetic energy dependence of escape depth (*28, 33*), for

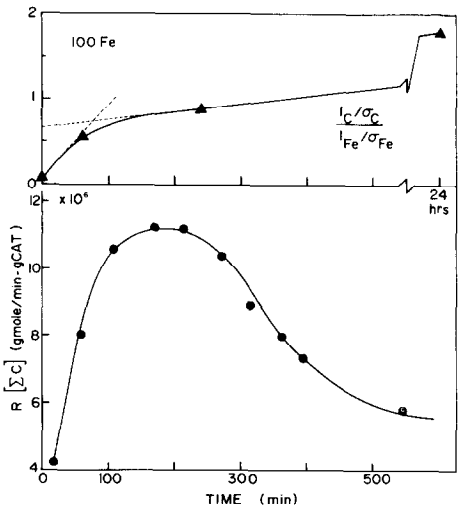

FIG. 6. Upper curve: Carbon incorporation on Fe during Fischer–Tropsch synthesis at 573°K as measured by XPS; lower curve: total hydrocarbon synthesis activity of Fe versus reaction time during Fischer–Tropsch synthesis at 573°K.

the C 1*s* and Fe $2p_{3/2}$ lines in the XPS spectra of Fe powders which have been pretreated in $3H_2/CO$ at 1 atm and 573°K for different times. As can be seen, there are two rate periods of carbon incorporation into the pure-Fe catalyst. The first rate period corresponds to formation of bulk iron carbide. The stoichiometry of the carbide calculated from the XPS data is $Fe_{1.5}C$ which is approaching agreement with the stoichiometry of χ carbide at $Fe_{2.5}C$. The slower rate period corresponds to the formation of a carbon overlayer on top of the carbide phase. The rate of carbon overlayer formation is much slower on the pure-Fe samples than on the 75Ru25Fe and 33Ru67Fe alloys. Recall that the carbon to metal ratio for the 75Ru25Fe catalyst treated for only 1 hr at 573°K was 3.9 as compared to a ratio of 1.8 on Fe after 24 hr at the same temperature. Examination of the SIMS yields from the reduced Fe catalyst and the same catalyst after 4 hr of Fischer–Tropsch synthesis at 573°K further supports this interpretation. For the 75Ru25Fe alloy, the metal ions nearly disappeared from the spectra after 1 hr of reaction because of the thick carbon overlayer formed. The growth of bulk iron carbide is evidenced in Fig. 7 by the slow decay of the Fe^+ yield. It is lower than for pure Fe because of dilution with carbon in the bulk, but is clearly visible because of minimal carbon overlayer formation.

TABLE 3

Selectivity Data for Fischer–Tropsch Synthesis over Fe Powder at 573°K[a]

Product	S_{C_n}	σ (%)
C_1	0.283	4.0
C_2	0.300	3.6
C_3	0.206	5.8
C_4	0.090	10

[a] S_{C_n} = fraction of CO converted which goes to the product indicated. σ = standard deviation over the first 200 min.

The formation of the carbide followed by the carbon overlayer on supported Fe is accompanied by the expected maximum in the rate of hydrocarbon production shown in the lower curve of Fig. 6. Remarkably, the hydrocarbon selectivities of the Fe catalyst remain essentially unchanged during the entire carburization process, as shown by the small standard deviations in Table 3. On the other hand, the selectivity of the catalyst to unsaturated products, Fig. 8, varies significantly during carbide formation. Interpretation of Fig. 8 is complicated by the fact that higher olefin production is accompanied by lower conversion. At this time we cannot accurately separate the roles of conversion and carbon deposition in determining olefin production. We note, however, that even after thick carbon overlayer formation at 573°K, the iron catalyst

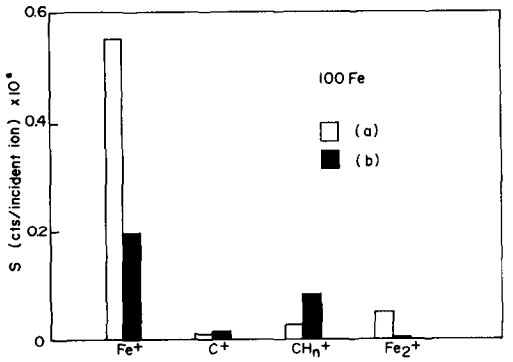

FIG. 7. Carbon incorporation on Fe during Fischer–Tropsch synthesis at 573°K as measured by SIMS: (a) reduced; (b) $3H_2/CO$, 4 hr, 573°K.

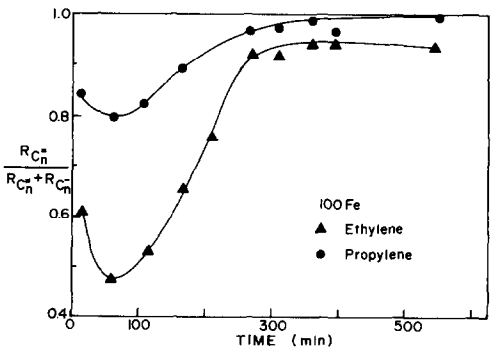

FIG. 8. Selectivity of the Fe catalyst to unsaturated hydrocarbons as a function of time on stream during Fischer–Tropsch synthesis at 573°K.

gave an ethylene to ethane ratio of 14 at 0.8% conversion. The overlayer growth was also accompanied by a shift in product distribution to lower-molecular-weight products as in the 75Ru25Fe and 33Ru67Fe cases.

CONCLUSIONS

The interactions of carbon from 1 atm of $3H_2/CO$ syngas with unsupported Ru, Fe, and RuFe alloys can be classified in three groups. Pure Ru and 97Ru3Fe exhibit less than 0.25 monolayer of carbon buildup during 24 hr of Fischer–Tropsch synthesis at 573°K. 75Ru25Fe and 33Ru67Fe alloys show rapid buildup of carbon during Fischer–Tropsch synthesis approaching a steady-state, equivalent thickness of around 40 Å. The carbon overlayer is unaffected by H_2 treatment at 603°K but is completely removed by H_2 at 683°K. Pure iron accepts carbon into the bulk and then carbon builds up slowly on the carbided iron.

Alteration in activity and selectivity of the catalyst for Fischer–Tropsch synthesis depends on the nature of the carbon interaction. Pure-Ru and 97Ru3Fe alloys catalyze the Fischer–Tropsch synthesis reaction at a uniform rate per surface atom. The hydrocarbon selectivity is also unchanged during the first 24 hr of reaction. The uniform kinetic behavior of this group is the result of minimal carbon deposition on the surface.

Carbon buildup on the 75Ru25Fe and 33Ru67Fe catalysts occurs on the time scale of hours. The multilayer deposition of carbon shifts selectivity of the catalyst toward lower-molecular-weight products. In addition, the specific activity of the catalyst declines by a factor of 2 to 3. Removal of the carbon overlayer by high-temperature H_2 treatment restores initial activity and selectivity patterns.

The unsupported iron catalyst accepts carbon into the bulk during the initial 24 hr on stream, along with a slow buildup of carbon on the surface. Carbide formation results in a temporary increase in hydrocarbon synthesis activity as well as changes in the olefin to paraffin selectivity. The hydrocarbon length selectivity, however, remains unchanged until carbon buildup on the surface is large.

ACKNOWLEDGMENTS

We are grateful to the National Science Foundation for support of this work by Grants CHE 78-08728 and DMR 77-23798. It is also a pleasure to thank N. Winograd and W. E. Baitinger for many enlightening discussions of this research and W. D. Kostka for obtaining the kinetic data on Ru powder.

REFERENCES

1. Ott, G. L., Fleisch, T., and Delgass, W. N., *J. Catal.* **60**, 394 (1979).
2. Fuggle, J. C., Umback, E., Feulner, P., and Menzel, D., *Surface Sci.* **64**, 69 (1977).
3. Fuggle, J. C., Madey, T. E., Speinkilberg, M., and Menzel, D., *Surface Sci.* **52**, 521 (1975).
4. Singh, K. J., and Grenga, H., *J. Catal.* **47**, 328 (1977).
5. Eastman, D. E., Demuth, J. E., and Baker, J. M., *J. Vac. Sci. Technol.* **11**, 273 (1974).
6. Low, G. C., and Bell, A. T., *J. Catal.* **57**, 397 (1979).
7. McCarty, J. G., and Wise, H., *Chem. Phys. Lett.* **61**, 323 (1979).
8. Rabo, J. A., Risch, A. P., and Poutsma, M. L., *J. Catal.* **53**, 295 (1978).
9. Dalla Betta, R. A., and Shelef, M., *J. Catal.* **48**, 111 (1977).
10. Ekerdt, J. G., and Bell, A. T., *J. Catal.* **58**, 170 (1979).
11. Broden, G., Gafner, G., and Bonzel, H. P., *Appl. Phys.* **13**, 333 (1972).
12. Brundle, C. R., *IBM J. Res. Develop.* **22**, 235 (1978).
13. Yoshida, K., and Somorjai, G. A., *Surface Sci.* **75**, 46 (1978).
14. Kishi, K., and Roberts, M. W., *J. Chem. Soc. Faraday Trans. I* **71**, 1715 (1975).
15. Yu, K. Y., Spicer, W. E., Lindau, I., Pianetta, P., and Lin, S. F., *Surface Sci.* **57**, 157 (1976).
16. Barber, M., Vickerman, J. C., and Wolstenholme, J., *Surface Sci.* **68**, 130 (1977).
17. Fleisch, T., Ott, G. L., Delgass, W. N., and Winograd, N., *Surface Sci.*, submitted.
18. Hofer, L. J. E., *in* "Catalysis," Vol. IV (P. H. Emmett, Ed.), p. 373. Reinhold, New York, 1956.
19. Anderson, R.B., *in* "Catalysis," Vol. IV (P. H. Emmett, Ed.), pp. 29, 257. Reinhold, New York, 1956.
20. Amelse, J. A., Butt, J. B., and Schwartz, L. H., *J. Phys. Chem.* **82**, 558 (1978).

21. Raupp, G. B., and Delgass, W. N., *J. Catal.* **58,** 348 (1979).
22. Hewitt, R. W., Shepard, A. T., Baitinger, W. E., Winograd, N., and Delgass, W. N., *Rev. Sci. Instrum.* **50,** 1386 (1979).
23. Fleisch, T., Shepard, A. T., Ridley, T. Y., Vaughn, W. E., Winograd, N., Baitinger, W. E., Ott, G. L., and Delgass, W. N., *J. Vac. Sci. Technol.* **15,** 1756 (1978).
24. Fleisch, T., Winograd, N., and Delgass, W. N., *Surface Sci.* **78,** 141 (1978).
25. Kostka, W. D., M.S. thesis, Purdue University, 1976.
26. Cusumano, J. A., and Garten, R. L., private communication.
27. Ott, G. L., Baitinger, W. E., Winograd, N., and Delgass, W. N., *J. Catal.* **56,** 174 (1979).
28. Scofield, J. H., *J. Electron Spectrosc.* **8,** 129 (1976).
29. McKee, D. W., *J. Catal.* **8,** 240 (1967).
30. Benninghoven, A., and Muller, A., *Surface Sci.* **39,** 416 (1973).
31. Harrison, D. E., Jr., Kelley, P. W., Garrison, B. J., and Winograd, N., *Surface Sci.* **76,** 311 (1978).
32. Fraser, W. A., Florio, J. V., Delgass, W. N., and Robertson, W. D., *Surface Sci.* **36,** 661 (1973).
33. Penn, D. R., *J. Electron Spectrosc.* **9,** 29 (1976).
34. Matsumoto, H., and Bennett, C. O., *J. Catal.* **53,** 331 (1978).
35. King, D. L., *J. Catal.* **51,** 386 (1978).
36. Fischer, F., and Dilthey, P., *Brennst. Chem.* **9,** 24 (1928).
37. Raupp, G. B., and Delgass, W. N., *J. Catal.* **58,** 361 (1979).